Comparative Study of the Rheological Behavior of Multiwalled Carbon Nanotubes and Nanofiber Composites Prepared by the Dilution of a Masterbatch of Polypropylene

T. Boronat,[1] D. Garcia-Sanoguera,[1] J. Pascual,[2] F. Peris,[2] L. Sanchez-Nacher[1]

[1]*Instituto de Tecnología de Materiales, Universitat Politècnica de València, Plaza Ferrándiz y Carbonell, s/n, Alcoy 03801, Spain*
[2]*Textile Technology Institute, Plaza Emilio Sala 1, Alcoy 03801, Spain*

Received 25 March 2011; accepted 1 December 2011
DOI 10.1002/app.36623
Published online in Wiley Online Library (wileyonlinelibrary.com).

ABSTRACT: In this investigation, the characteristics and the rheological properties of two different nanocomposite systems were investigated. These systems consisted of a dispersion of carbon nanotubes (CNTs) and carbon nanofibers (CNFs) in a polypropylene (PP) matrix. The mixing process was carried out by melt compounding with a twin-screw corotating extruder with different reinforcement amounts (0.2–20 wt %) from concentrated masterbatches (20 wt %) of PP/CNT and PP/CNF. The results show a remarkable increase in the viscosity for both blends as the reinforcement amount was increased. It was important to evaluate the rheological behavior to understand the effect of the nanocarbon particles on the internal structures and their processing properties of the obtained composites. CNFs were a more viable reinforcement from a processability point of view because the obtained viscosities of the PP/CNF blends were more manageable. © 2012 Wiley Periodicals, Inc. J Appl Polym Sci 000: 000–000, 2012

Key words: carbon nanotube; nanocomposites; poly(propylene) (PP); rheology

INTRODUCTION

Polypropylene (PP) is a thermoplastic polymer that is used in a wide variety of applications because of the combination of its low cost and its excellent properties, including stiffness, chemical resistance, low specific gravity, and good mechanical properties. PP has been substituted for other polymers, such as poly(vinyl chloride), polyurethanes, and polyethylene, in a wide range of applications. However, PP's processability into foams or films is very difficult because of its low melt strength. The addition of fillers to PP to improve its mechanical properties has been widely investigated. Recently, nanometer-scale reinforcing particles have attracted considerable attention from polymer scientists, and they have been used to substitute for traditional fillers and fibers in polymer matrices. The most common reinforcements at the nanoscale include inorganic clay minerals consisting of silicate layers, such as those mentioned by LeBaron et al.[1]

Correspondence to: T. Boronat (tboronat@dimm.upv.es).
Contract grant sponsor: Universitat Politècnica de València; contract grant number: PAID-06-10-003-300.

Carbon nanotubes (CNTs) and carbon nanofibers (CNFs) are a rather novel class of nanomaterials and are widely used as reinforcements for polymers. CNTs are made of carbon, where the basic unit is a graphitic plane rolled to form a hollow cylinder, whose diameter is on the order of a few nanometers. On the other hand, CNFs are considered as intermediate materials between conventional carbon fibers and CNTs. CNFs have been developed to produce nanometer-sized carbon fibers as an alternative to nanotubes. CNFs are cheaper, and it is possible to produce them in large volumes. CNFs have generated great interest as a result of their many possible applications; that is why recent efforts have been directed toward their optimization and their production on an industrial level.

Although both reinforcements are carbon-based, their crystalline structures are very different. On one hand, CNTs are the third crystalline form of carbon. CNTs are basically just a tube made from hexagonally bonded carbon. Multiwalled nanotubes consist of multiple rolled layers (concentric tubes) of graphite. In contrast, CNFs can be defined as amorphous carbon fibers, that is, fibers without a defined crystal structure, but in fact, they are aggregated filamentous graphite microparticles that are randomly distributed.[2] The crystalline structure is an important

issue because processing conditions are strongly dependent on it.

Both materials are very interesting for researchers because of their excellent mechanical properties, high thermal and electrical conductivity, and great stability at high temperatures. Because of their good characteristics, high aspect ratio (surface/area ratio), and low density, they may be used as reinforcements in substitution of traditional fillers in polymer matrices. Manchado et al.[3] used single-walled CNTs as mechanical reinforcement for PP composites prepared by melt processing. Because of their high aspect ratio, CNTs present the advantage of being able to be added to the polymer at very low concentrations to obtain improvements in the mechanical characteristics. The addition of CNFs to a polymer also improves the mechanical characteristics. Zhou et al.[4] developed a homogeneous mixture of SC-15 epoxy resin and CNFs. The tensile and flexural strengths were compared to those of the composite without CNFs; improvements of 11 and 22.3%, respectively, were obtained.

The electrical properties also are improved with the addition of nanotubes, Allaoui et al.[5] quantified that the transition from insulator to conductor in composite samples took place for nanotube concentrations between 0.5 and 1 wt %. Another study by the same research group[6] determined that the insulator-to-conductor transition region spanned about one order of magnitude, from 0.1 to 1 wt %, when CNFs were used as fillers. In another study, Bauhofer and Kovacs[7] analyzed the electrical percolation in CNT polymer composites. Byrne and Gun'ko[8] studied both the electrical and mechanical properties; they tabulated the most recent values of Young's modulus and the electrical conductivity for various CNT–polymer composites and compared the effectiveness of different processing techniques. A recent study by Li et al.[9] demonstrated that simultaneously strengthened and toughened nanocomposites based on a PP/ethylene–propylene–diene monomer thermoplastic elastomer matrix could be achieved through enhanced adhesion between multiwalled carbon nanotubes (MWCNTs) and the polymer matrix with PP-grafted MWCNTs.

The addition of CNTs to PP also affects the thermal properties. Logakis et al.[10] observed that the crystallization temperature peak shifted gradually to higher temperatures as the amount of CNTs was increased. The observed increase in the crystallization temperature was more pronounced at low nanotube contents and became weaker as the amount of CNTs was increased. Additionally, the crystallization peak appeared to be narrower in the case of the nanocomposites, and a slight increase in the degree of crystallinity was also observed as the amount of CNTs was increased. Very little information is available with regard to the influence of CNFs on the thermal properties of thermoplastic polymers. Lozano and Barrera[11] reported an increase in the thermal stability of PP in the presence of CNFs.

Many studies[12–14] have been carried out on improving the dispersion of CNTs/CNFs in polymers and the adhesion between the filler and the polymer matrix. Methods including chemical modification, polymer chain wrapping, ultrasonication, and the aid of surfactants have been adopted.

In contrast, there have been no studies that examined the rheological behavior of carbon nanoparticles on PP, although rheology is a very important feature in polymer processing. The objective of this investigation was to evaluate the influence of the rheological properties of different quantities of either CNTs or CNFs in a PP matrix.

EXPERIMENTAL

Materials

Composite materials were produced by the mixture of PP as the base polymer both with CNTs and carbon nanofibers (CNFs). The base polymer was a commercial homopolymer-grade PP (Moplen HP561s); it was supplied by Basell Polyolefins (Basell Poliolefinas Iberica S. L., Tarragona, Spain). The base material has a melt flow rate (MFR) of 33 g of·(10 min)$^{-1}$; this makes it suitable for production of continuous filaments by extrusion. Typical applications of Moplen HP561s are high-tenacity yarns and spunbond nonwovens.

On the one hand, the matrix polymer was mixed with commercial Nanocyl-7000 series thin MWCNTs. The nanotubes used in this work were manufactured by a carbon vapor deposition process supplied by Nanocyl (Nanocyl S. A., Sambreville, Belgium).

On the other hand, another composite material was prepared. The same PP grade as before was used to prepare the new composite, but this time, it was filled with CNFs. The fibers used are commercially known as Grupo Antolin carbon nanofibers (GANFs), and they were provided by Antolin Engineering Group (Burgos, Spain). GANFs are submicrometer vapor-grown carbon fibers. The product technical data provided by the suppliers for both fillers is shown in Table I.

Composite fabrication

The same procedure was used to prepare both composites (PP/CNT and PP/CNF). The starting material was a masterbatch previously prepared with 20 wt % filler via melt compounding. The dilution was done in a corotating extruder (model ZSK 18 Mc, Werner & Pfleiderer, Stuttgart, Germany), which was provided with two gravimetric side feeders. The pressure used

TABLE I
Filler Technical Data

Property	Method of measurement	CNTs	CNFs
Fiber diameter (nm)	TEM	8–10	20–80
Fiber length (μm)	TEM	1.5	>30
Graphitization degree (%)	Thermogravimetric analysis	90	70
Metallic particle content (%)	Thermogravimetric analysis	10	6–8
Surface area (m^2/g)	Brunauer–Emmett–Teller	250–300	100–200

was 19 bar, and the selected temperature profile was 200–220–220–220–220–200–200–220–220–220–220–220°C from the pellet inlet to the extruder head. A very exhaustive control of the temperature of the melt was applied to prevent overheating, as this would produce degradation in the material. The screw rate applied was 500 rpm, and the feed rate obtained was 10 kg/h with a measured melt temperature at the extruder head of 213°C.

Once the two masterbatches were prepared, different dilutions were obtained by their mixture with pure PP. The same processing conditions and the same extruder as those used in the masterbatch production were used to prepare the dilutions. The obtained concentrations varied within the range 0.2–20 wt % (i.e., 0.2, 0.5, 1.0, 2.0, 3.0, 4.0, 5.0, 10.0, and 20.0 wt %).

Rheological characterization

The steady-shear flow behavior of the dilutions was measured with a capillary rheometer, model Rheoflixer MT from Thermo Haake (Karlsruhe, Germany) at 210 and 220°C. Five minutes were allowed for the material to reach the intended temperature after the barrel was charged. The rheometer was equipped with three separate dies, all of them with 1-mm diameters and die length-to-diameter ratios (L/D's) of 10, 20, and 30, respectively. The shear rates were varied between 100 and 10000 s^{-1}. The tests were performed according to ISO-11443. The viscosity values for each die corresponded to the average of the five experimental tests.

Microscopic characterization

The microscopic analysis of the compounds was carried out in a JEOL instrument, model JEM-2010 (Peabody, Massachusetts). To cut the samples for transmission electron microscopy (TEM) characterization, an ultramicrotome (RMC model MTXL) under cryogenic conditions was needed because PP is a soft polymer.

Methodology of the viscosity calculation

The apparent viscosity (η_{ap}) of a polymer in the molten state can be easily obtained with capillary rheology with the following equations at a constant temperature:

$$\eta_{ap} = \frac{\tau_{ap}}{\gamma_{ap}}$$

$$\tau_{ap} = \frac{P \cdot D}{4 * L}$$

where τ_{ap} is the apparent shear stress (Pa), γ_{ap} is the apparent shear rate (s^{-1}), P is the test pressure at the die inlet (bar), D is the die diameter (mm), and L is the length of the die (mm).

An overpressure is caused by the pass of the molten material from a greater (barrel) to a lesser diameter (die); this alters the direct obtained results from the rheometer. This overpressure can be determined and corrected with the Bagley correction. The application of this methodology requires one to obtain the pressure at the die inlet with three dies with different L/D values at diverse shear rates (100, 200, 500, 1000, 2000, 5000, and 10,000 s^{-1}). So, the real shear stress (τ_{real}; Pa) was calculated with the Bagley equation:

$$\tau_{real} = \frac{-P}{4\left(\frac{L}{D} + e\right)}$$

where P is the test pressure at the die inlet (bar) and e is the additional apparent die length equivalent to the overpressure (mm).

The experimental results were corrected for non-Newtonian effects with the Rabinowitsch correction to determine the real shear rate (γ_{real}; s^{-1}) that was applied to the polymer. The slope of the log γ_{ap} versus log τ_{real} plot was calculated by adjusting the curve to a third-degree polynomial:

$$\gamma_{real} = \frac{\gamma_{app}}{4}\left(3 + \frac{d\log\gamma_{app}}{d\log\tau_{real}}\right)$$

where $\frac{d\log\gamma_{app}}{d\log\tau_{real}}$ is the slope of the curve.

Once both real parameters are calculated, the real viscosity can be easily calculated:

$$\eta_{real} = \frac{\tau_{real}}{\gamma_{real}}$$

Rheological model fit

The parameters of the Cross–Williams–Landel–Ferry (Cross–WLF) rheological model were determined to develop a deeper analysis. The Cross model[15] was chosen to assess the viscosity of the material because it fit well to the behavior of the studied compounds at high shear rates. For a proper fit at low shear rates, it was necessary to supplement the Cross model with the WLF model[16] because it allowed us to determine the value of the viscosity under zero-shear-rate conditions. It also enabled us to determine the influence of the temperature on the shear viscosity.

The expression of the Cross model as function of shear rate is as follows:

$$\eta = \frac{\eta_0}{1 + \left(\frac{\eta_0 \cdot \dot{\gamma}}{\tau^*}\right)^{(1-n)}}$$

where η_0 is the material viscosity under zero-shearrate conditions (Pa s), τ^* is the model constant that shows the shear stress rate from which the pseudoplastic behavior of the material starts (Pa), $\dot{\gamma}$ is the applied shear rate (1/s), and n is the power law coefficient of the Cross model that symbolizes the pseudoplastic behavior slope of the material as $1 - n$. The temperature dependence was introduced through the function η_0, which takes the WLF form and enables one to determine the viscosity of the material under zero-shear-rate conditions:

$$\eta_0 = \begin{cases} D_1 \cdot e^{\left(\frac{-A_1 \cdot (T-\tilde{T})}{A_2 + (T-\tilde{T})}\right)}, & \text{if } T \geq \tilde{T} \\ \infty, & \text{if } T < \tilde{T} \end{cases}$$

$$A_2 = \tilde{A}_2 + D_3 \cdot p$$

$$\tilde{T} = D_2 + D_3 \cdot p$$

A_2 is a model parameter which depends from the studied material and from the dependece of the glass-transition temperature from pressure, T is the applied temperature (k), p is the pressure (Pa) where $\tilde{T}$ is the glass-transition temperature of the material (K), depending on the pressure, D_2 is the model constant that registers the glass-transition temperature of the material at atmospheric pressure (K), D_3 characterizes the linear pressure dependence of the glass-transition temperature of the material according to the pressure (K/Pa), D_1 is the model constant that registers the material viscosity under zero-shear-rate conditions at the material glass-transition temperature and at atmospheric pressure (Pas), A_1 is the model constant that shows the temperature dependence of the material glass-transition temperature under zero-shear-rate conditions, and $\tilde{A}_2$ is a model parameter that depends on the type of material that is being considered (K).

Reig et al.[17] developed an adjustment that determines the Cross–WLF model parameters from the experimental results. The seven model parameters are handled in two groups according to the dependence on the material's physical properties. In this study, the constant values were assigned to the three independent parameters of the material:

$$\tilde{A}_2 = 51.6K$$

$$D_2 = T_g = -30C = 243.15K$$

$$D_3 = \partial T_g / \partial p = 0.25 \times 10^6 K/Pa$$

The other four parameters were dependent on the material's physical properties and were calculated with Reig's methodology.

RESULTS AND DISCUSSION

The effect of CNTs/CNFs on the internal structure and processing properties of the filled PP was studied through analysis of the rheological properties of the obtained composites in the molten state. Rheological measurements are very sensitive to the shape, size, surface area, crystalline structure, and dispersion of the fillers in nanocomposites. Figure 1 shows the viscosity curves of the pure PP and PP/CNT composites measured at 210°C as function of the shear rate (which ranged from 10^2 to 10^4 s^{-1}). The viscosity curves of the PP/CNT melts exhibited non-Newtonian behavior in the entire shear rate range. The behavior was shear thinning in the entire studied range; this showed a large dependence of the viscosity on the shear rate. The pure PP curve showed at low shear rates a less pseudoplastic behavior; as the CNTs content was increased, the shear thinning behavior was extended to lower shear rates. The shear thinning behavior of the material could be associated with the alignment of the tubes along the flow direction. The viscosity increased with the nanotube content because of the interaction between the PP matrix and the nanotubes. The effect of the nanotubes was most pronounced at a low shear rate, and the relative effect diminished with increasing shear rate because of shear thinning. The η_0 value of the PP/CNTs increased from 386.5 to 12,087.9 Pa s at 210°C as the loading on the CNTs increased from 0 to 20 wt %.

The viscosity of the blends increased as the CNT content increased because of the high specific surface area, backbone rigidity, porosity, and agglomerates of the CNTs, which prevented the composite melt from flowing. So, the melt processing of the highly concentrated CNT/PP composites would be difficult because of the extremely high viscosity because the viscosity of the PP/CNT composite melt was sensitive to CNT loading.[18] This effect is more pronounced in the transformation processes that

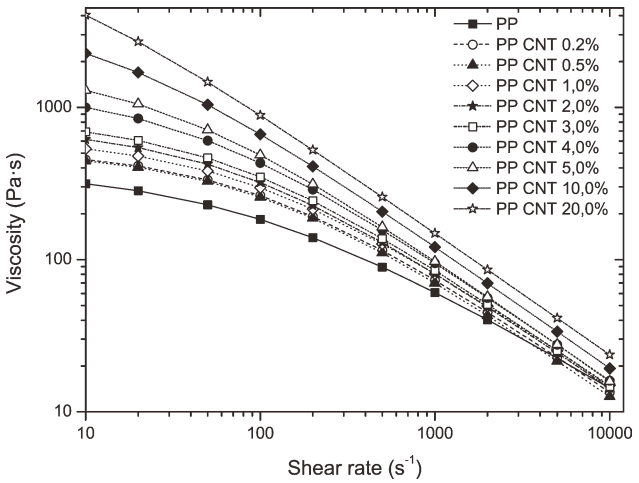

Figure 1 PP/CNT viscosity curves (210°C).

work at low shear rates such rotational molding or thermoforming. However, the effect is less important in transformation processes that work with very high shear rates, such as injection molding, because the differences of the viscosity values decrease as the shear rate increases.

Rheological tests also were performed on the CNF compounds with the same loads by weight that were applied to the CNT composites. Figure 2 shows the viscosity of the PP/CNF compounds as a function of the shear rate at 210°C. At low shear rates, the viscosities of the highly concentrated PP/CNF blends presented lower values than the same blend of CNTs because the specific surface area and aspect ratio of the CNFs were lower than those of the CNTs. The crystal structure of the filler also had to be considered; the cylindrical structure of the CNTs increased the viscosity of the blends compared to the CNF blends for the same concentration of filler. Even though an increasing viscosity could be observed with higher CNF loadings, the observed shear thinning effect seemed not to be strongly dependent on the amount of fibers. The issue of the processing of nanoreinforced systems disappeared at high shear rates as the viscosity was reduced in magnitude, and the nanocomposite viscosity tended toward the matrix viscosity.

Figure 3 confirms the influence of the temperature on the shear viscosity. The shear viscosity decreased with increasing shear rate at a constant temperature. As the temperature was increased, the shear viscosity of the compounds was reduced. It was important to understand the viscosity sensitivity to temperature, as it heavily influenced the processing conditions and the quality of the final products. The increase in the temperature caused a decrease in the intermolecular or intramolecular resistance associated with the viscosity and produced more thermal motion of the molecules and, thus, a greater free volume in the polymer.[16]

Table II shows the values of the four dependent parameters of the Cross model obtained and the η_0 calculated values at 210°C for all of the studied composites. D_1 was not considered as a relevant parameter because it represented the viscosity at the glass-transition temperature and zero-shear-stress conditions; this was a very different process condition from that applied in this study. However, D_1 was determined to calculate η_0 with the WLF expression.

A_1 shows the viscosity sensitivity to temperature. Materials with a high A_1 value show a higher temperature sensitivity of viscosity. The evolution of A_1 behavior versus the amount of both additives is shown in Figure 4. In both cases, there was a downward trend in the A_1 value when the amount of additive in the composite was increased. Thus, the increase of filler reduced the sensitivity to temperature, especially when the material was reinforced with nanotubes. The PP/CNT melts showed a sustained decline in the A_1 parameter with increasing

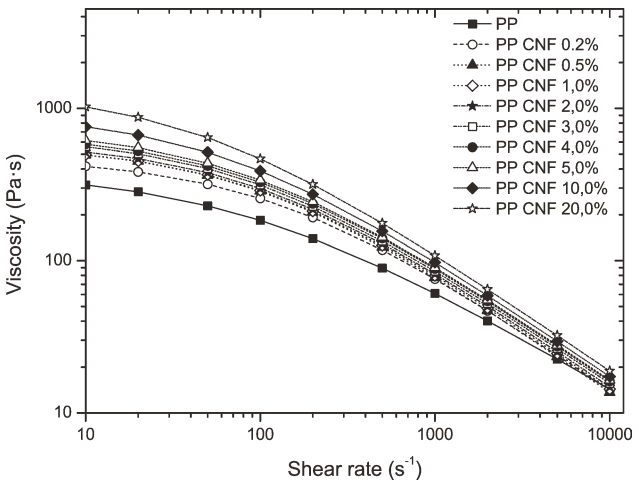

Figure 2 PP/CNF viscosity curves (210°C).

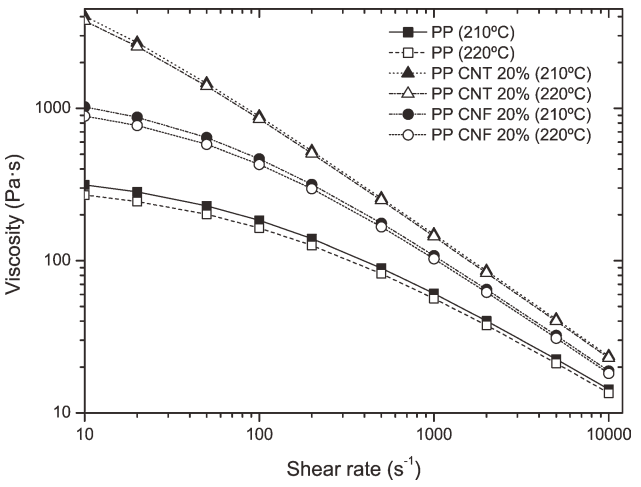

Figure 3 Viscosity curves showing the influence of temperature.

TABLE II
Cross–WLF Dependent Parameters of the PP/CNT and PP/CNF Composites

	A_1	D_1 (Pa s)	τ (Pa)	n	η_0 (Pa s; 210°C)
PP	29.97	1.993×10^{13}	3.354×10^4	0.3138	386.5
PP/CNTs 0.2%	29.04	1.270×10^{13}	5.199×10^4	0.2114	529.4
PP/CNTs 0.5%	30.54	4.278×10^{13}	5.067×10^4	0.2021	517.9
PP/CNTs 1.0%	28.95	1.417×10^{13}	5.368×10^4	0.2192	635.0
PP/CNTs 2.0%	29.69	3.058×10^{13}	5.213×10^4	0.2068	748.1
PP/CNTs 3.0%	29.54	3.066×10^{13}	5.401×10^4	0.2014	848.8
PP/CNTs 4.0%	27.82	1.173×10^{13}	5.304×10^4	0.2023	1328.9
PP/CNTs 5.0%	27.64	1.418×10^{13}	5.124×10^4	0.1930	1865.7
PP/CNTs 10.0%	27.52	2.777×10^{13}	5.419×10^4	0.1927	4044.5
PP/CNTs 20.0%	25.94	2.269×10^{13}	5.114×10^4	0.1976	12,087.9
PP/CNFs 0.2%	29.19	1.283×10^{13}	5.845×10^4	0.2072	473.6
PP/CNFs 0.5%	29.42	1.870×10^{13}	5.743×10^4	0.1930	571.1
PP/CNFs 1.0%	29.37	1.811×10^{13}	5.821×10^4	0.2022	575.1
PP/CNFs 2.0%	29.23	1.682×10^{13}	5.904×10^4	0.2045	601.1
PP/CNFs 3.0%	29.34	2.025×10^{13}	5.840×10^4	0.2132	660.2
PP/CNFs 4.0%	29.17	1.831×10^{13}	6.104×10^4	0.2107	685.5
PP/CNFs 5.0%	29.04	1.761×10^{13}	6.027×10^4	0.2134	733.7
PP/CNFs 10.0%	28.89	1.968×10^{13}	6.128×10^4	0.2113	927.6
PP/CNFs 20.0%	28.60	2.227×10^{13}	6.084×10^4	0.2128	1332.9

reinforcement content. The range for the CNTs between the maximum value (virgin material) and the minimum value was 4.60 for the A_1 value, so there was a loss of sensitivity with increasing reinforcement amount. The PP/CNF composites presented a very slight drop in this value; there was only a difference of 1.37 in the A_1 values between that of pure PP and that of the blend with the highest percentage of reinforcement (20%). Therefore, the variation of temperature sensitivity in the PP/CNFs was negligible. The effect of temperature sensitivity cannot be appreciated in Figure 3 because the A_1 parameter presented low values, and the temperature difference applied was not high enough to manifest the CNT sensitivity. Table III confirms that the effect of temperature over viscosity was greater with low levels of reinforcement. So, the amount of filler reduced the temperature sensitivity, especially for the CNT filler. Anyway, the loss of sensitivity was negligible because there was only a 2% difference between PP with no load and PP with a load of 20% of CNTs.

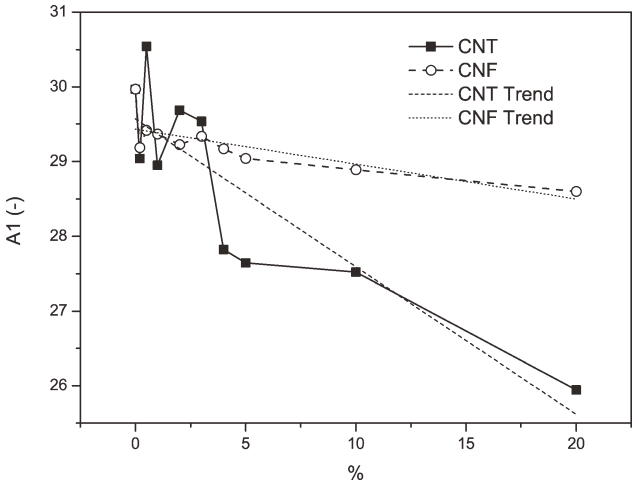

Figure 4 Variation of A_1 in terms of the reinforcement charge.

η_0 was considered a consistent parameter, although it was calculated with the A_1 and D_1 parameters because it was measured at 210°C. η_0 was an important parameter in the cooling phase of the extrusion processes, where the material did not flow. Figure 5 shows the upward trend of η_0 with the increasing content of reinforcement material. There were very different behaviors for the two types of reinforcement. The η_0 values for low levels of reinforcement were similar, but when the concentration exceeded 4 wt %, the CNT blend values increased exponentially. In contrast to that of the PP/CNF blends, the viscosity increase was more sustained and fit to a line. η_0 for the 20 wt % PP/CNT blends was nine times higher than of the PP/CNF blend. This result corroborated the difference in the viscosity between the curves of Figures 1 and 2. This was caused by the larger specific surface

TABLE III
Percentage Changes in the Viscosity from 210 to 220°C

Amount of filler (%)	CNTs	CNFs
0	−16.12	−16.12
0.2	−15.67	−15.74
0.5	−16.41	−15.85
1.0	−15.62	−15.83
2.0	−15.99	−15.76
3.0	−15.91	−15.81
4.0	−15.06	−15.73
5.0	−14.97	−15.67
10.0	−14.91	−15.59
20.0	−14.12	−15.45

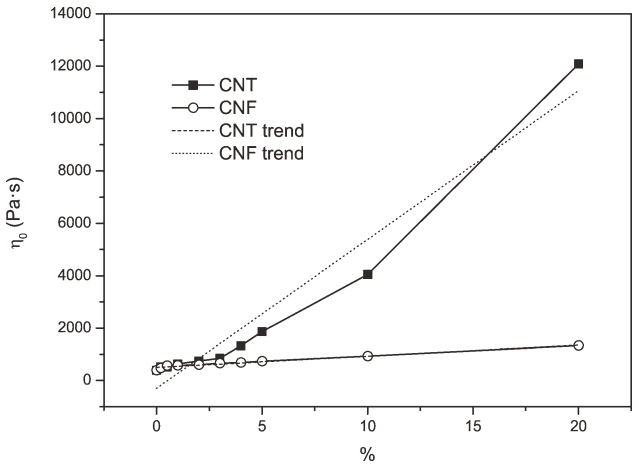

Figure 5 Variation of η_0 in terms of the reinforcement charge.

area of the CNTs, which increased the suspension viscosity because of the high hydrodynamic interactions between the particles.

Parameter τ represents the shear stress at which the onset of the shear thinning behavior occurred. It is an important parameter because it determines the transition between the Newtonian and the shear thinning regime. Figure 6 clearly shows that τ increased with the addition of the reinforcing material to the PP matrix, either CNTs or CNFs. The increase in τ extended the Newtonian regimen, so there was a higher region where the shear rate did not affect the viscosity, and as a consequence, the viscosity was higher. This harmed the processing. The PP-loaded materials tended to stabilize the value of τ, regardless of load level. The PP/CNT bends presented an average τ value of 52,454 Pa, whereas in the PP/CNF blends, the average was 59,439 Pa.

The value of $1 - n$, where n is the power law coefficient in the Cross model, represents the slope of the shear thinning region. Newtonian fluids present n values equal to 1. From a processability point of view, it is interesting to handle low n values to get lower viscosities at the same shear rate. Figure 7 shows that pure PP had higher values of n than the studied blends. The value of n in the blends tended to stabilize around an average value, as with the τ parameter; this showed that the pseudoplastic behavior was not affected by the quantity of nanotubes or nanofibers. It was just modified by their presence. The CNTs affected the behavior of the PP more because they reduced the value of n more. The value of n in the virgin material was 0.314. It decreased to an average value of 0.203 in the PP/CNT blends, and in the PP/CNF blends, the average value was 0.208.

Figure 8 shows microphotographs of the PP/CNT composites. In such images, the internal structure of this kind of blend can be observed. In blends with low contents of CNTs, there was a fairly homogeneous fine dispersion of the CNTs in the PP matrix. As the nanotube content increased, the internal structure of the blend varied, and the dispersed density of the CNTs increased in the PP matrix [Fig. 8(c,d)]. For these nanotube particle concentrations, we observed a trend toward the formation of small clusters of nanotubes. As the amount of CNTs increased, some segregation was observed [Fig. 8(e,f)]. Individual CNTs or small clusters were homogeneously dispersed together with large CNTs aggregates and could be clearly distinguished [Fig. 8(f)]. This meant that the melt mixing of the CNTs on the polymer matrix did not lead to the total dispersion of the CNTs, and this effect was more pronounced with high CNTs contents. The CNT particles were evenly dispersed in the PP matrix as individual CNTs, small CNTs clusters, or large CNT aggregates, which made the flow of the polymer chains of the thermoplastic material difficult; in other words, the viscosity increased.

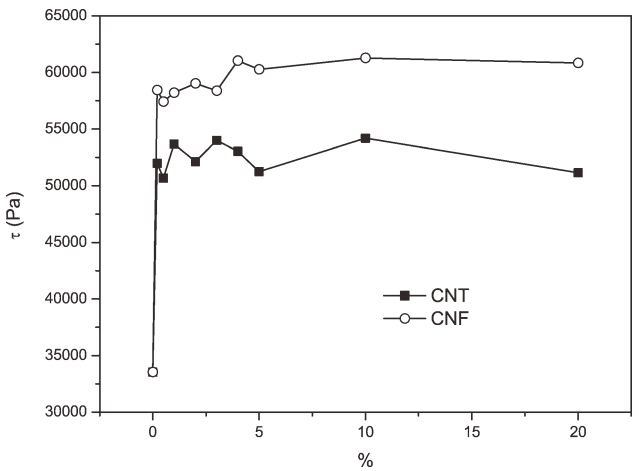

Figure 6 Variation of τ in terms of the reinforcement charge.

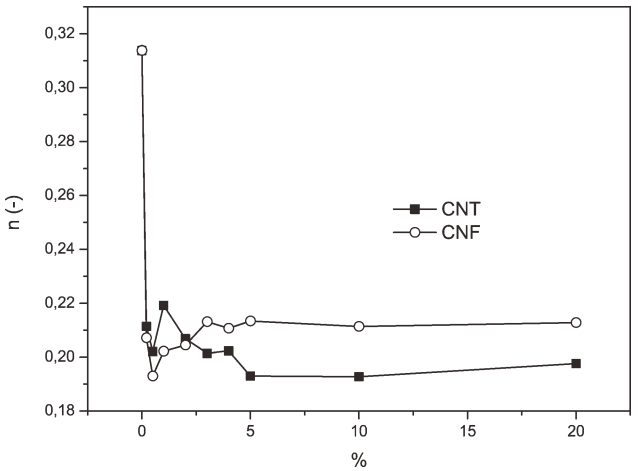

Figure 7 Variation of n in terms of the reinforcement charge.

Similarly, the PP composites with CNFs changed their behavior with increasing content of nanofibers. The increase in the viscosity due to the rise in CNF content was directly related to the change in the internal structure of the PP polymer. Figure 9 shows TEM micrographs of the PP/CNF blends at 12,000×. For low contents of CNF (0.2 and 0.5%), individual nanofibers uniformly dispersed in the polymer matrix were observed. When the content of CNFs was increased, the density also increased considerably with a homogeneous dispersion. The same phenomenon was observed for high levels of CNFs [Fig. 9(e,f)]; there were dense structures in the dispersed phase with uniform and regular distribution. The presence of this dispersed phase of CNFs in the polymer matrix prevented the flow of the thermoplastic polymer chains, so the CNTs acted as reinforcements, and consequently, the viscosity directly increased with the amount of CNFs.

However, it is interesting to note that the dispersed phase in the PP/CNT blends was much smaller than that in the PP/CNFs. The nanotubes that we used had diameters of 8–10 nm, and the nanofibers had diameters of 20–80 nm, whereas the lengths ranged from 1.5 μm for the CNTs and above 30 μm for the CNFs. The greater surface area presented by the CNTs compared to the CNFs provided a greater area of interaction between the reinforcement and the PP matrix; this produced an anchoring effect of the polymer chains to the carbon particles, which prevented slide between them. This was analyzed quantitatively and showed a much higher increase in viscosity for the PP/CNT systems than for the PP/CNFs for the same content by weight.

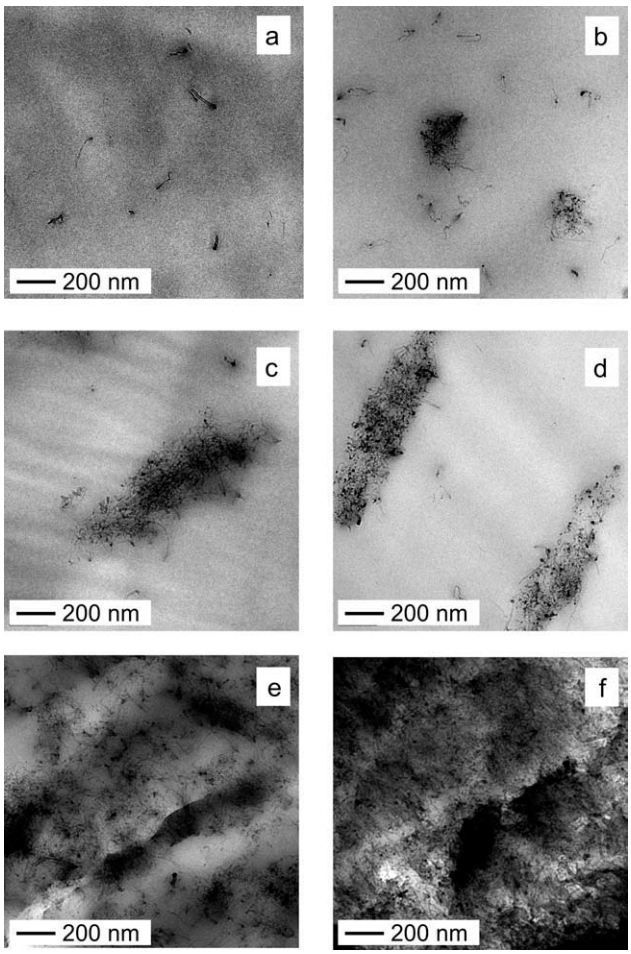

Figure 8 TEM microphotographs (12,000×) of the PP–CNT compounds with different CNT weight percentages: (a) 0.2, (b) 0.5, (c) 1, (d) 2, (e) 10, and (f) 20%.

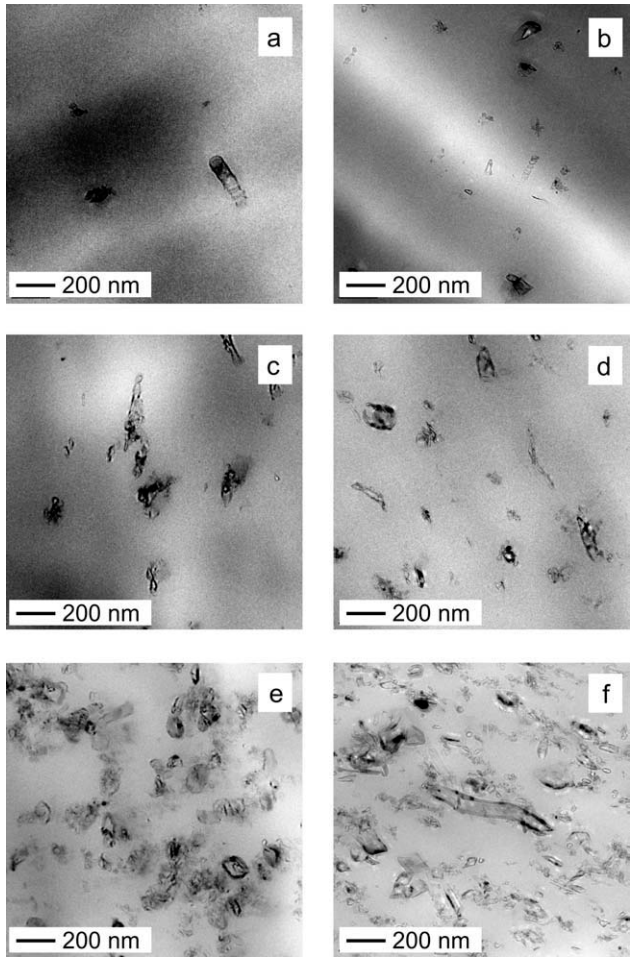

Figure 9 TEM microphotographs (12,000×) of the PP–CNF compounds with different CNF weight percentages: (a) 0.2, (b) 0.5, (c) 1, (d) 2, (e) 10, and (f) 20%.

CONCLUSIONS

In this work, the effects of carbon nanoreinforcements on the rheology were studied, both in nanotube and nanofiber formats. These two reinforcements were evaluated to evaluated CNFs as an economical substitute for CNTs. The results show that the reinforced

PP presented higher viscosity values than the pure material, especially the CNT blends. The addition of reinforcement particles produced a significant variation in the rheological behavior. The viscosity curves moved up, showing an increasing viscosity. The pseudoplastic zone varied its behavior; the onset of the shear thinning zone was shifted to higher values of shear stress, and the slope was reduced. Therefore, the processing of the reinforced materials was more difficult, especially in the polymer manufacturing processes, which worked at low shear rates.

The viscosity values of the reinforced materials were compared, and we observed that the CNT blends had much higher viscosities than the CNF blends. This difference was due to the fact that the CNTs had a larger specific surface area and higher backbone rigidity and microporosity; these increased the suspension viscosity because of increased hydrodynamic interactions between the particles. This phenomenon increased with the percentage of CNTs added; this made its processing very difficult with high concentrations of CNTs. So if a reinforced material with high thermal or mechanical performance is needed, it would be better to use CNFs from the standpoint of processability. The high viscosity of the blends with high CNT loadings were reduced slightly because of the high sensitivity that these blends had to the temperature.

In addition, the reinforced materials presented stable behavior in the pseudoplastic phase, regardless of the additive loading. This was corroborated by the behavior of the Cross model parameters that characterized this phase (τ and n).

The authors thank to R. Boronat for linguistic assistance.

References

1. LeBaron, P. C.; Wang, Z.; Pinnavaia, T. J. Appl Clay Sci 1999, 15, 11.
2. Davis, W. R.; Slawson, R. J.; Rigby, G. R. Nature 1953, 171, 756.
3. Manchado, M. A. L.; Valentini, L.; Biagiotti, J.; Kenny, J. M. Carbon 2005, 43, 1499.
4. Zhou, Y.; Pervin, F.; Jeelani, S.; Mallick, P. K. J Mater Process Technol 2008, 198, 445.
5. Allaoui, A.; Bai, S.; Cheng, H. M.; Bai, J. B. Compos Sci Technol 2002, 62, 1993.
6. Allaoui, A.; Hoa, S. V.; Pugh, M. D. Compos Sci Technol 2008, 68, 410.
7. Bauhofer, W.; Kovacs, J. Z. Compos Sci Technol 2009, 69, 1486.
8. Byrne, M. T.; Gun'ko, Y. K. Adv Mater 2010, 22, 1672.
9. Li, C.; Deng, H.; Wang, K.; Zhang, Q.; Chen, F.; Fu, Q. J Appl Polym Sci 2011, 121, 2104.
10. Logakis, E.; Pollatos, E.; Pandis, Ch.; Peoglos, V.; Zuburtikudis, I.; Delides, C. G.; Vatalis, A.; Gjoka, M.; Syskakis, E.; Viras, K.; Pissis, P. Compos Sci Technol 2010, 70, 328.
11. Lozano, K.; Barrera, E. V. J Appl Polym Sci 2001, 79, 125.
12. Zhang, Y. C.; Broekhuis, A. A.; Stuart, M. C. A.; Landaluce, T. F.; Fausti, D.; Rudolf, P.; Picchioni, F. Macromolecules 2008, 41, 6141.
13. O'Bryan, G.; Yang, E. L.; Zifer, T.; Wally, K.; Skinner, J. L.; Vance, A. L. J Appl Polym Sci 2011, 120, 1379.
14. Bose, S.; Khare, R. A.; Moldenaers, P. Polymer 2010, 51, 975.
15. Cross, M. M. J Colloid Sci 1965, 20, 417.
16. Williams, M. L.; Landel, R. F.; Ferry, J. D. J Am Chem Soc 1955, 77, 3701.
17. Reig, M. J.; Segui, V. J.; Zamanillo, J. D. J Polym Eng 2005, 25, 435.
18. Lee, S. H.; Kim, M. W.; Kim, S. H.; Youn, J. R. Eur Polym J 2008, 44, 1620.